

Aft-End Design Techniques for Twin-Engine Fighters

Edsel R. Glasgow* and Don M. Santman†

Lockheed-California Company, Burbank, Calif.

Techniques for designing the aft-end of fighter aircraft having twin buried engines and dual nozzles were developed using the thrust and drag results obtained from an experimental and analytical investigation of various twin-nozzle/aftbody configurations. Predesign guidelines were formulated for use in developing or modifying aircraft aft-end arrangements so that a high thrust minus drag can be achieved. Also, post-design methods for predicting the aft-end drag of the final aircraft designs were developed. These design techniques were utilized to improve five selected baseline configurations. Mission analysis studies were conducted to determine the tradeoff between engine thrust, aircraft weight, and external drag for three different mission profiles. Improvements in mission radius for a fixed aircraft takeoff gross weight were obtained by modifying the baseline configurations to include convergent-divergent nozzles, a horizontal wedge interfairing with the trailing edge terminating at the exit plane of the nozzles, and a single vertical stabilizer.

Nomenclature

A	= area
A_E	= twin nozzle exit area
A_{MAX}	= maximum fuselage cross-sectional area
A_{MB}	= fuselage cross-sectional area at wing trailing edge (metric break) station
A_S	= nozzle boattail cross-sectional area at nozzle exit station
C_{DAE}	= aft-end pressure drag coefficient based on projected frontal area, $A_{MB} - A_S$
C_{DEB}	= equivalent body pressure drag coefficient based on projected frontal area, $A_{MAX} - A_S$
C_{DBT}	= total boattail pressure drag coefficient based on projected frontal area, $A_{MAX} - A_S$
C_T	= nozzle thrust coefficient based on inviscid one-dimensional analysis and referenced to ideal gross thrust, F_{ID}
D_{MAX}	= equivalent diameter corresponding to an area of a circle equal to the maximum fuselage cross-sectional area, A_{MAX}
D_{MB}	= equivalent diameter corresponding to an area of a circle equal to the fuselage cross-sectional area at metric break station, A_{MB}
F_G	= nozzle thrust based on inviscid one-dimensional analysis
F_{ID}	= nozzle ideal gross thrust based on isentropic expansion of ideal mass flow to ambient pressure
IMS	= integral mean slope for boattail surface between maximum fuselage area and nozzle exit stations

$$-1/(1 - A_E/A_{MAX}) \int_{A_E/A_{MAX}}^1 [d(A/A_{MAX})/d(X/D_{MAX})] d(A/A_{MAX})$$

$IMSA$ = integral mean slope for boattail surface between metric break and nozzle exit stations

$$-1/(1 - A_E/A_{MB}) \int_{A_E/A_{MB}}^1 [d(A/A_{MB})/d(X/D_{MB})] d(A/A_{MB})$$

$IMSI$ = integral mean slope for boattail surface between maximum fuselage area and metric break stations

$$IMS(A_{MAX} - A_S)/(A_{MAX} - A_{MB}) - IMSA(D_{MB}/D_{MAX})(A_{MB} - A_S)/(A_{MAX} - A_{MB})$$

Presented as Paper 72-1111 at the AIAA/SAE 8th Joint Propulsion Specialist Conference, New Orleans, La., November 29-December 1, 1972; submitted December 8, 1972; revision received October 9, 1973. This work was sponsored by the Air Force Flight Dynamics Laboratory under Contract F33657-70-C-0511.

Index category: Aircraft Configuration Design; Aircraft Performance; Airbreathing Propulsion, Subsonic and Supersonic.

*Research Specialist, Member AIAA.

†Senior Propulsion Engineer.

M_∞	= freestream Mach number
P_E	= nozzle exit static pressure
P_L	= nozzle boattail static pressure at nozzle exit station
q_L	= nozzle boattail dynamic pressure at nozzle exit station
X	= distance
ΔD	= drag increment
θ_E	= nozzle boattail trailing edge angle

Introduction

THE achievement of proper airframe/nozzle integration has become significantly more difficult and important with the advent of the multimission aircraft requiring variable geometry nozzles to operate over a broad range of altitudes and Mach numbers. The mutual interactions that occur between the nozzle exhaust and the external flowfield can alter the pressure distributions on the aft-end of the fuselage and produce both internal and external flow separation. Such interactions can result in significant penalties in both aircraft drag and engine thrust. It has been difficult in the past to minimize these losses because adequate analytical methods and empirical information were not available during the aircraft design phase.

In order to improve this situation, a 32-month program was initiated in 1969 for the development and assembly of design techniques for producing improved nozzle installations.^{1,2} This experimental and analytical program has examined isolated nozzle/aftbody configurations³⁻⁵ and twin-nozzle/airframe installations.⁶⁻⁸ During the isolated nozzle model tests, large scale (eight inch diameter) convergent, convergent-divergent, and plug nozzles were investigated. An evaluation of analytical and empirical methods for predicting the thrust and drag of these nozzle configurations has been discussed previously.⁹ During the twin-jet tests, the same nozzles were installed in a generalized model of an advanced air superiority fighter having twin buried engines and dual nozzles (Fig. 1). The airframe design was selected from among those developed by General Dynamics under contract with the Air Force Flight Dynamics Laboratory.¹⁰

Presented in this paper are the aft-end design techniques developed from the thrust and drag results obtained during the twin-jet tests. The following configuration variables were examined over a 0.6 to 2.5 Mach number range during this test program: nozzle type, power setting position, lateral spacing, and axial position; fuselage fairing contour; horizontal stabilizer area and deflection; vertical stabilizer type, longitudinal position, area,

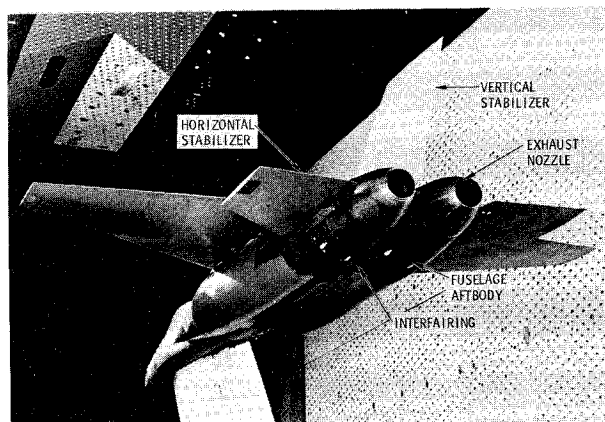


Fig. 1 Twin-jet test rig installation.

and rudder deflection; and interfairing type, length, height, and base area. Predesign guidelines were formulated for use in developing or modifying aircraft aft-end arrangements so that high thrust minus drag can be achieved. Also, post-design methods for predicting the aft-end drag of the completed aircraft designs were developed. These techniques were used to modify the aft-end design of five selected aircraft configurations, and the mission radius for a fixed TOGW (takeoff gross weight) was employed as the criteria for evaluating the design improvements.

Predesign Guidelines

Considerable time and expense is involved in developing a layout of a new or modified fighter configuration and in evaluating the design using mission analysis results. In order to minimize the number of configurations subjected to the complete design process, predesign guidelines have been formulated for screening candidate aft-end arrangements prior to developing a layout of the designs. These guidelines consist of a listing of the recommended configurations for each of the aft-end components identified in Fig. 1 (i.e., exhaust nozzle, interfairing, fuselage aftbody, and horizontal and vertical stabilizers). The aft-end component configurations were selected from among those investigated during the twin-jet tests. The criterion used in selecting these configurations was that of maximizing the thrust minus aft-end drag. The aft-end drag, which was obtained from both pressure and force balance data, includes the forces on all external surfaces aft of the wing trailing edge (metric break) station except for those on the stabilizers.

The predesign guidelines are listed in Table 1. The guidelines are divided into two main categories: one for aircraft mission carried out primarily at subsonic and transonic Mach number with no augmentation required for most segments and the other for aircraft missions carried out primarily at supersonic Mach numbers with augmentation required. The experimental results used in formulating the guidelines are discussed briefly below.

The differences in thrust minus aft-end drag due to nozzle type result primarily from differences in aft-end drag at subsonic speeds and in nozzle thrust coefficient at supersonic speeds. The long, smooth contours of convergent iris and convergent-divergent nozzles are pressurized by the nozzle flow at subsonic speeds, which diminishes the aft-end drag. The sharp corner on convergent flap nozzles and short turn at the end of the shroud of unshrouded plug nozzles prevent the nozzle flow from pressurizing the boattail area and result in no drag reduction for these nozzles. At supersonic speeds, the thrust coefficients are higher for convergent-divergent and unshrouded plug nozzles, which have flow expansion surfaces, than for

Table 1 Design Guidelines

RECOMMENDED AFT-END COMPONENTS	AIRCRAFT MISSION CATEGORIES	
	SUBSONIC - TRANSONIC	SUPERSONIC
NOZZLE TYPE	CONVERGENT IRIS OR CONVERGENT-DIVERGENT	CONVERGENT-DIVERGENT OR UNSHROUDED PLUG
NOZZLE SPACING	NOT CRITICAL	MINIMUM
INTERFAIRING TYPE	HORIZONTAL WEDGE	HORIZONTAL OR VERTICAL WEDGE
INTERFAIRING TRAILING EDGE LOCATION	NOZZLE EXIT PLANE	NOZZLE EXIT PLANE
VERTICAL STABILIZER	SINGLE	SINGLE
FUSELAGE CONTOURS AND AREA DISTRIBUTION	SMOOTH AREA DISTRIBUTION AVOID SHARP CORNERS AND STEPS	SMOOTH AREA DISTRIBUTION AVOID SHARP CORNERS AND STEPS MINIMIZE BOATTAIL ANGLE AND PROJECTED FRONTAL AREA

convergent nozzles, whose thrust coefficients decrease monotonically with increasing nozzle pressure ratio.

Nozzle lateral spacing has little effect on thrust at all speeds and on aft-end drag at subsonic speeds. At supersonic speeds, however, an increase in nozzle lateral spacing results in a significant aft-end drag increase. This drag increase is due to a reduction in the extent of flow separation and an increase in aft and forward facing frontal areas resulting from outboard displacement of the engine nacelles for attainment of increased nozzle spacing.

The aft-end drag for horizontal wedge interfairing configurations is significantly lower than that for vertical wedge interfairing configurations at subsonic speeds and approximately the same at supersonic speeds. The high drag for vertical wedge interfairing is due to the low pressure region between the interfairing and the normal power nozzle boattail. The aft-end drag decreases at all speeds as the interfairing trailing edge moves downstream from the nozzle attachment station to the exit plane of the convergent-divergent nozzles. Longer interfairings were tested for only the normal power convergent-divergent nozzle, and a minimum aft-end drag existed for the interfairing terminating at the nozzle exit plane. The type and length of interfairings employed have little effect on the nozzle thrust coefficients.

The aft-end drag for single vertical stabilizer configurations is significantly lower than that for twin vertical stabilizer configurations. The position of the twin vertical stabilizers on the aftbody, out of the flowfield plane of symmetry, results in greater flow disturbances and higher drag than for the plane-of-symmetry single vertical stabilizers. The type of vertical stabilizer employed has no effect on the nozzle thrust coefficient.

The cross-sectional area distribution of the aft-end should be smooth, avoiding sharp corners and steps, at all speeds. For supersonic flow, the aft-end drag increases significantly with increasing boattail angle and projected frontal area. As a result, these parameters should also be minimized.

Post-Design Drag Prediction Methods

Analytical and empirical techniques for predicting the thrust and aft-end drag of twin-engine fighter configurations were examined. Although several analytical methods are available which provide reasonably accurate aft-end pressure distribution trends, the predicted pressure levels are not sufficiently good to permit accurate drag calculations. For this reason, the empirical correlations of the drag data obtained during the twin-jet tests are recommended for use in predicting aft-end performance.

Examination of the model data obtained during this program indicates that isolated nozzle internal performance prediction methods described in Ref. 9 are applicable to twin-nozzle installations. This conclusion is based on the observation that the nozzle external flow did not significantly influence the internal flow. Some external flow influence (unsymmetrical interaction) on the plug nozzle performance was obtained for nozzle pressure ratios less than approximately 4.0. However, this unsymmetrical

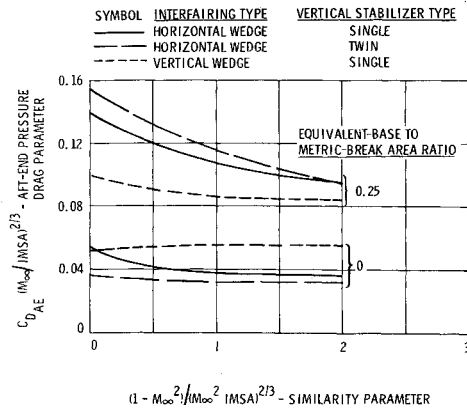


Fig. 2 Transonic similarity correlation of twin-jet drag—nozzle design pressure ratio.

interaction effect is not significant since the nozzle pressure ratios are greater than 4.0 for most fighter aircraft missions.

Subsonic External Flow

The drag correlations for subsonic external flow were developed in two parts: a correlation of the aft-end drag for operation at the nozzle design pressure ratio, and a correlation of the drag increment from design pressure ratio operation to operation at a higher nozzle pressure ratio. The design pressure ratio for convergent and convergent-divergent nozzles is defined as that total to ambient static pressure ratio associated with critical throat flow where the nozzle exit static pressure is equal to the ambient pressure. For unshrouded plug nozzles, the design pressure ratio is set equal to the design pressure ratio of a convergent nozzle. Since operation at nozzle pressure ratios lower than design pressure ratio is not often encountered for most fighter aircraft missions, drag correlations for these conditions were not developed.

A correlation of the aft-end drag for operation at the nozzle design pressure ratio is presented in Fig. 2 for configurations with horizontal or vertical wedge interfairings and a single vertical stabilizer or configurations with horizontal wedge interfairings and twin vertical stabilizers. The correlation was developed by combining Spreiter's transonic similarity parameters¹¹ with the integral mean slope of the equivalent body of revolution for the twin-jet models, IMSA. The correlation results are presented in the figure for two equivalent-base to metric-break area ratios where the equivalent-base area is defined as the difference between the boattail cross-sectional area at the nozzle exit and the nozzle exit flow area. Correlation results are provided for only two equivalent-base to metric-break area ratios since the aft-end pressure drag parameter of Fig. 2 varies linearly with area ratio for a constant value of the similarity parameter. Further, this linear variation was found to be the same for all three nozzle lateral spacings investigated.

The equivalent-base to metric-break area ratio is a measure of the amount of external flow recompression occurring over the aft-end. For example, at low equivalent base area ratios, the exhaust jet is in close proximity to the external flow at the nozzle exit resulting in a relatively large amount of external flow recompression on the aft-end and consequent relatively low drag forces. At large equivalent base area ratios, the external flow recompression effect occurs downstream of the aft-end and results in relatively high drag forces.

The method used for correlating the aft-end drags for nozzle pressure ratios greater than design is based on subsonic potential flow theory. In accordance with this theo-

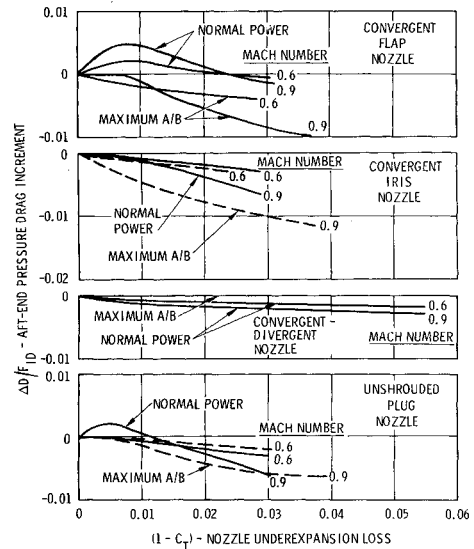


Fig. 3 Correlation of drag increment from design to higher operating nozzle pressure ratios.

ry, the net axial pressure force acting on the streamline adjacent to the aircraft surface must be equal (but opposite in direction) to the pressure force acting on the jet boundary. Assuming the exhaust jet does not influence the flowfield upstream of the aftbody, a change in the force acting on the exhaust plume boundary, due to a change in the nozzle pressure ratio, must be balanced by a change in the force acting on the aftbody and nozzle. The ideal axial force acting on the jet boundary, ΔD , can be determined by a momentum balance on the jet for a control volume beginning at the nozzle exit and extending downstream to infinity where the jet momentum is equal to the ideal thrust. Expressed algebraically

$$F_{ID} - F_G + \Delta D = 0 \quad (1)$$

In coefficient form, the above equation can be expressed as

$$(1 - C_T) + (\Delta D/F_{ID}) = 0 \quad (2)$$

While the idealizations involved render the above expression inaccurate on an absolute basis, it does strongly suggest that changes of drag, i.e., increments in drag from a reference drag, may be correlated with the nozzle underexpansion losses $(1 - C_T)$. The reference drag selected is the drag associated with the nozzle operating at its design pressure ratio.

The correlation of the drag increment from design pressure ratio operation to operation at a higher nozzle pressure ratio is presented in Fig. 3 for convergent flap, convergent iris, convergent-divergent, and unshrouded plug type nozzles. The correlation results for each nozzle type are Mach number and power setting dependent.

Supersonic External Flow

An equivalent body correlation was developed for supersonic external flow which consists of correlating the jet-off total drag aft of the maximum area station as a function of calculated equivalent body drag. The maximum area station was chosen as a reference station since the Mach number at this station is more nearly equal to the free-stream Mach number. The total drag for this procedure is the sum of the measured aft-end drag and the computed initial boattail drag for the region between the maximum area and metric break stations. All computed drags are obtained from Fig. 4 as a function of Mach number, mini-

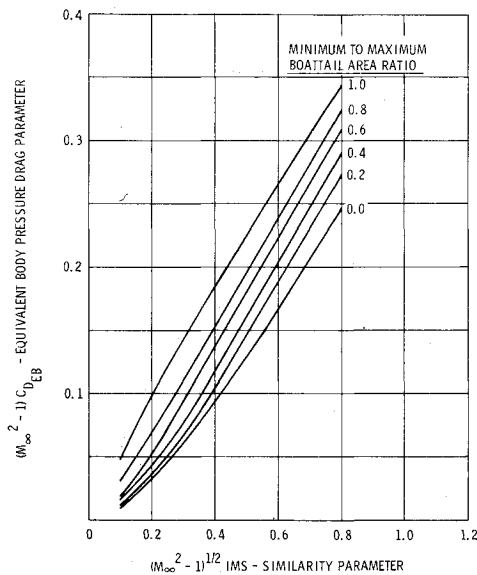


Fig. 4 IMS/supersonic similarity correlation of conical boattail MOC pressure drag.

imum to maximum fuselage area ratio, and integral mean slope—IMS for the equivalent body drag and IMSI for the initial boattail drag.

Figure 4 presents a correlation of conical boattail pressure drag coefficients (referenced to projected frontal area) obtained by use of the MOC (method of characteristics) for exit to maximum area ratios ranging from 0.0 (limiting case of a closed axisymmetric body) to 1.0 (limiting case of a two-dimensional boattail contour). Correlation of the data for a given area ratio is achieved through use of similarity parameters which are obtained from linearized supersonic flow theory. The MOC drag data used in generating the curves for each area ratio shown in Fig. 4 includes data for boattail angles ranging from three to nine degrees and Mach numbers ranging from 1.2 to 2.0. Although the data shown in Fig. 4 were generated from MOC solutions for conical boattails, the results are applicable for arbitrary boattail contours since, for a given area ratio, the IMS parameter accounts for the contour effect, as discussed in Ref. 1.

Jet-off drag correlations obtained by application of the above procedure to the data of this program are presented in Fig. 5 for Mach numbers of 1.2, 1.6, and 2.0, respectively. The jet-off data shown in the figure are for configurations with different nozzle types at maximum A/B (convergent iris, convergent flap, convergent-divergent, and unshroud plug), different interfairing types (horizontal

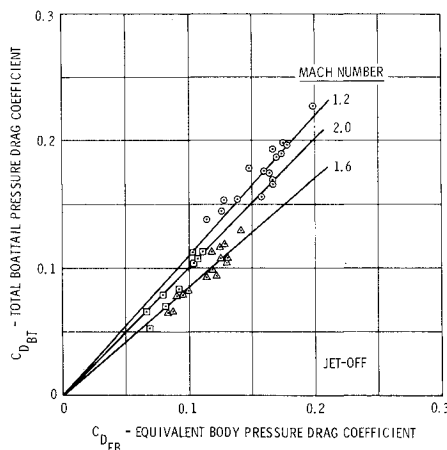


Fig. 5 Supersonic equivalent body drag correlation of twin-jet data—single vertical stabilizer configurations.

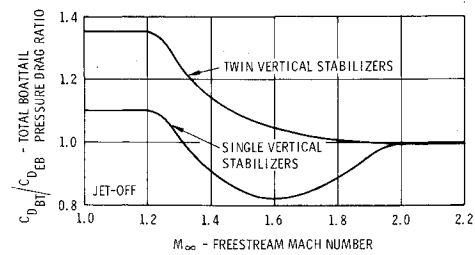


Fig. 6 Comparison of supersonic equivalent body drag correlation results for single and twin vertical stabilizer configurations.

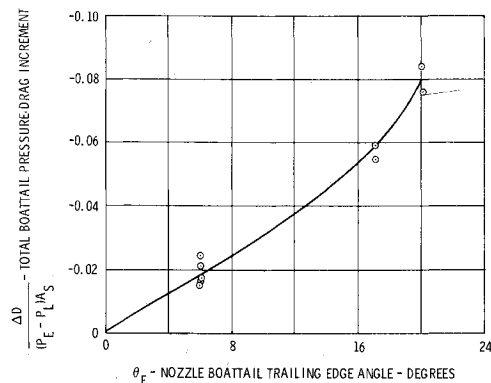


Fig. 7 Correlation of jet-on minus jet-off drag increment—supersonic flow.

and vertical wedge), and single vertical stabilizers. The data for each Mach number are correlated quite well by a straight line. If twin rather than single vertical stabilizers are employed, the equivalent body drag results must be adjusted by the amount indicated in Fig. 6.

To supplement the jet-off correlations presented above, a jet-on boattail drag correlation was developed and is presented in Fig. 7. The pressure drag increments (jet-on minus jet-off) normalized by the product of the shroud exit area (jet plus base area) and the difference between the nozzle internal and external static pressures (assuming no flow separation) are correlated as a function of nozzle boattail angle at the nozzle exit. The test data presented in the figure are for freestream Mach numbers of 1.2 and 1.6 and for the maximum A/B power setting unshrouded plug, convergent flap, and convergent iris nozzle configurations. The external nozzle boattail static pressure, P_L , used in the correlations was determined from MOC calculations. The correlation results are applicable for pressure coefficients, $(P_E - P_L)/q_L$, greater than 1.4 and for supersonic Mach numbers less than 2.0. Little or no flow separation occurs for values outside the indicated limits, as determined from empirical observation.

Application of Design Techniques

Mission analysis studies have been used in developing and selecting twin-nozzle/afbody installations. Initially, five baseline configuration were selected from among those tested during the program. The engine thrust, aircraft weight, and external drag for each selected design was then predicted and used in determining the aircraft mission radius for a fixed TOGW of 45,000 lb. Next, the aft-end lines of each baseline configuration were modified so that an improved candidate installation would result. The rationale for these modifications was derived from an analysis of the baseline mission results, predesign guidelines developed during the program, and specified design constraints. The new design was considered to be an improved installation if its mission radius was greater than that of the corresponding baseline configurations.

Table 2 General Arrangement of Baseline Configurations

AFT-END COMPONENTS	X-1	X-2	X-3	X-4	X-5
NOZZLE TYPE	CONVERGENT-DIVERGENT	CONVERGENT-DIVERGENT	CONVERGENT-DIVERGENT	CONVERGENT FLAP	CONVERGENT-DIVERGENT EJECTOR
NOZZLE EXPANSION	PREDETERMINED	PREDETERMINED	PREDETERMINED	--	PREDETERMINED
NOZZLE SPACING	NARROW	INTERMEDIATE	WIDE	NARROW	NARROW
INTERFAIRING TYPE	VERTICAL WEDGE	HORIZONTAL WEDGE	HORIZONTAL WEDGE	HORIZONTAL WEDGE	HORIZONTAL WEDGE
INTERFAIRING TRAILING EDGE LOCATION	NOZZLE EXIT STATION	NOZZLE EXIT STATION	NOZZLE EXIT STATION	CUSTOMER CONNECT STATION	CUSTOMER CONNECT STATION
VERTICAL STABILIZER	SINGLE	SINGLE	TWIN	SINGLE	SINGLE
FUSELAGE AIRBODY SHAPE	NON-AREA-RULED	NON-AREA-RULED	NON-AREA-RULED	NON-AREA-RULED	NON-AREA-RULED

Baseline Configuration Selection

The general arrangement of each of the five selected baseline configurations (X-1 through X-5) is identified in Table 2. This group of configurations provide an interesting matrix in that the primary configuration variables investigated during the test program, viz., nozzle type and spacing, interfairing type and length, and vertical stabilizer type, are all represented. All baseline configurations have a high wing, half-axisymmetric inlets mounted on the sides of the fuselage forward of the wing leading edge, the same forebody, and close coupled stabilizers.

The X-1 configuration, which has a narrow nozzle spacing and vertical wedge interfairing, closely resembles the initial F-111 design and for this reason was chosen as a baseline configuration. A simulation of the F-111 aft-end was considered important since the F-111 was the most advanced fighter in production at the beginning of the contracted effort. Also, the airframe-nozzle integration problems encountered with the F-111 provided the primary impetus for initiating this and several other propulsion research programs.

The X-2 design, which has an intermediate nozzle spacing and a horizontal wedge interfairing with the trailing edge terminating at the exit plane of the convergent-divergent nozzles, was selected since it represents a design intermediate between the X-1 and X-3 configurations. The latter configuration is somewhat similar to the F-14 in that it has a wide nozzle lateral spacing, horizontal interfairing, and twin vertical stabilizers.

The X-4 and X-5 configurations are identical except for the choice of nozzles. They both are narrow spaced configurations and have horizontal wedge interfairings with the trailing edge terminating at the nozzle attachment point (customer connect station). These configurations were selected so that the tradeoff between nozzle performance and weight could be evaluated. The performance of the convergent flap nozzles installed in the X-4 configuration has been compromised in order to reduce nozzle weight. A higher weight of the convergent-divergent ejector nozzle installed in the X-5 configuration has been accepted in order to obtain better performance.

Candidate Configuration Development

The baseline configurations were modified to improve their thrust and aft-end drag characteristics. The new designs were considered only candidates for improvement since whether or not they are indeed improvements is dependent on the tradeoff between performance and weight, as subsequently determined from the mission analysis studies. The general arrangement of the three candidate configurations which evolved (Y-1 through Y-3) is identified in Table 3.

The Y-1 configuration is the candidate developed for improving the performance of the X-1, X-4, and X-5 baseline configurations. Replacing the vertical interfairing of the X-1 configuration with a horizontal wedge interfairing

Table 3 General Arrangement of Candidate Configurations

AFT-END COMPONENTS	Y-1	Y-2	Y-3
NOZZLE TYPE	CONVERGENT-DIVERGENT	CONVERGENT-DIVERGENT	CONVERGENT-DIVERGENT
NOZZLE EXPANSION	OPTIMUM	OPTIMUM	OPTIMUM
NOZZLE SPACING	NARROW	NARROW	WIDE
INTERFAIRING TYPE	HORIZONTAL WEDGE	HORIZONTAL WEDGE	HORIZONTAL WEDGE
INTERFAIRING TRAILING EDGE LOCATION	NOZZLE EXIT STATION	NOZZLE EXIT STATION	NOZZLE EXIT STATION
VERTICAL STABILIZER	SINGLE	SINGLE	SINGLE
FUSELAGE AIRBODY SHAPE	AREA RULED	EXTENDED WITH NO VOLUME REDUCTION	REDUCED AREA BETWEEN NOZZLES

reduces the aft-end drag, especially at subsonic speeds, with only an 8 lb increase in weight. The aft-end drag of the X-4 and X-5 configurations is reduced in the Y-1 configuration by increasing the interfairing length such that the interfairing trailing edge terminates at the exit plane of the convergent-divergent nozzles instead of at the nozzle customer connect station. This increase in length results in a 20 lb weight penalty, but allows the vertical stabilizer to be located further aft on the aircraft. This results in a 144 lb weight reduction since a smaller vertical stabilizer having the same effectiveness can be utilized. The convergent-divergent nozzle installed in the Y-1 configuration, which is 300 lb heavier than the convergent flap nozzle installed in the X-4 configuration and 360 lb lighter than the convergent-divergent ejector nozzle installed in the X-5 configuration, is considered a potential overall improvement since it represents a compromise in both weight and performance. Further improvements were obtained by area ruling the portion of the fuselage aft of the maximum cross-sectional area station and by adjusting the nozzle expansion to obtain maximum thrust minus aft-end drag.

The Y-2 configuration was developed to illustrate that the aft-end drag can be reduced by decreasing the nozzle spacing and increasing the aft-end length of the X-2 configuration, while keeping the volume of the two aircraft the same. This results in a higher fineness ratio and therefore lower drag with a 551 lb increase in fuselage weight. The area of the horizontal and vertical stabilizers was reduced to maintain the same stabilizer effectiveness utilized for all previous configurations, which results in a 439 lb weight reduction. The nozzle expansion was again adjusted to maximize thrust minus aft-end drag.

The X-3 configuration was modified by removing area between the nozzles, substantially reducing the height of the horizontal wedge interfairing, and replacing the twin vertical stabilizers with a single vertical stabilizer. A 147 lb weight penalty is associated with increasing the aircraft wetted area by carving out cross-sectional area while maintaining the same nozzle lateral spacing. A 333 lb weight improvement, however, was obtained by replacing the twin vertical stabilizer with a single vertical stabilizer. The cross-sectional area distribution for the resultant Y-3 configuration is equivalent to that of the intermediate-spaced X-2 configuration. Further improvements were obtained by adjusting the nozzle expansion to obtain maximum thrust minus aft-end drag.

Improved Design Selection

The performance of the five baseline configurations (X-1 through X-5) and the three candidate configurations (Y-1 through Y-3) has been analyzed in three different Air Force missions. These include: 1) Basic Air Superiority Mission which consists of only subsonic segments with no augmentation required, 2) Tactical Air-Air Mission, which consists of one transonic segment at maximum augmented power and all other segments at subsonic speeds

Table 4 Comparison of Baseline and Candidate Configurations

PARAMETER	Y-1 MINUS X-1 INCREMENT	Y-2 MINUS X-2 INCREMENT	Y-3 MINUS X-3 INCREMENT	Y-1 MINUS X-4 INCREMENT	Y-1 MINUS X-5 INCREMENT
MISSION RADIUS - PERCENT					
BASIC AIR SUPERIORITY MISSION	+ 6.30	+ 0.89	+ 10.57	- 4.92	+ 19.30
TACTICAL AIR-AIR MISSION	+ 9.30	+ 1.94	+ 16.76	- 7.07	+ 19.77
SUPERSONIC POINT INTERCEPT MISSION	+ 2.59	+ 11.78	+ 24.84	+ 20.77	+ 8.68
ZERO FUEL WEIGHT-POUNDS	+ 8.0	+ 112	+ 186	+ 170	+ 456
AFT-END DRAG COEFFICIENT					
MACH 0.9, NORMAL POWER	- 0.00120	+ 0.00078	- 0.00020	+ 0.00036	- 0.00047
MACH 1.2, MAXIMUM A/B	- 0.00085	- 0.00066	- 0.00144	- 0.00069	- 0.00078
MACH 2.2, MAXIMUM A/B	- 0.00017	- 0.00181	- 0.00104	- 0.00254	- 0.00101
NOZZLE THRUST COEFFICIENT					
MACH 0.9, NORMAL POWER	+ 0.0003	+ 0.0041	+ 0.0019	+ 0.0019	- 0.0005
MACH 1.2, MAXIMUM A/B	+ 0.0002	+ 0.0007	+ 0.0002	+ 0.0017	- 0.0008
MACH 2.2, MAXIMUM A/B	+ 0.0	+ 0.0	+ 0.0	+ 0.0475	- 0.0235

with no augmentation required, and 3) Supersonic Point Intercept Mission, which consists primarily of supersonic segments with augmentation required. The takeoff gross weight was held constant for all designs at 45,000 lb. For the Tactical Air-Air Mission, two 200-gallon, tip-mounted fuel tanks were used which increased the takeoff gross weight to 47,900 lb. Weapon armament consisted of 4 semisubmerged Sparrow missiles, an internal gun, and ammunition. Combat fuel allowance for all missions is that fuel necessary to gain 144,000 ft of maneuver energy utilizing maximum power at 0.9 Mach number and 10,000-ft altitude.

The mission radius for each vehicle design was computed for all three mission profiles using a digital computer program designed to work from basic data such as drag polars, thrust minus power setting dependent inlet and aft-end drags, and fuel flow tables. The procedures used for computing these inputs are described in considerable detail in Ref. 1. The methods used to determine the aft-end drags have been discussed previously. The fuel flow requirements for an advanced technology turbofan engine, which was installed in all configurations, were obtained from a computer performance deck.

The mission radius increments associated with the modifications to the baseline configurations are itemized in Table 4 for each of the three missions analyzed. The corresponding increments in the zero fuel weight and the aft-end drag and nozzle thrust at three important mission points are also presented.

The mission radii of the Y-1, Y-2, and Y-3 candidate configurations are greater than those of the X-1, X-2, and X-3 baseline configurations, respectively, for all three missions investigated. The lower drag and higher thrust of the Y-1 and Y-2 configurations over that of the X-1 and X-2 configurations, respectively, more than compensated for the associated weight penalty. Although the indicated subsonic aft-end drag for the narrow-spaced Y-2 configuration is greater than that for the intermediate-spaced X-2 configuration, the total aircraft drag of the Y-2 configuration is less due to nozzle lateral spacing effects. The thrust, drag, and weight of the Y-3 configuration were all better than that of the X-3 configuration. Based on the mission analysis results, configurations Y-1, Y-2, and Y-3 are considered improvements over configurations X-1, X-2, and X-3, respectively.

The thrust and drag of the Y-1 configuration are better than those for the X-4 configuration for transonic and supersonic conditions only. As a result of these performance trends and the zero fuel weight penalty, the mission radius for the Y-1 configuration is greater than that for the X-4 configuration only for the supersonic point intercept mission. Therefore, the determination of whether the Y-1 design is an improvement over the X-4 design depends on the mission profile being considered.

The lower drag and lower zero-fuel weight of the Y-1 configuration over that of the X-5 configuration more than compensated for the lower nozzle thrust. Consequently, the mission radius for the Y-1 configuration is greater for all three missions investigated. Configuration Y-1 is therefore considered an improvement over configuration X-5.

Conclusions

An experimental and analytical investigation of the installed thrust and drag of various twin-nozzle/aftbody configurations indicated that empirical correlations provide the best means of predicting aft-end performance, especially for the early stages of the aircraft design. However, several analytical methods were available which provided reasonably accurate aft-end pressure distribution trends.

A correlation of twin-nozzle/aftbody drag at subsonic and transonic speeds was developed by combining IMSA with Spreiter's transonic similarity parameters. Twin-nozzle/aftbody drag data at supersonic speeds was correlated with the equivalent body drag obtained from a correlation of inviscid MOC pressure drag. This axisymmetric MOC correlation was achieved through use of IMS combined with similarity parameters obtained from linearized supersonic flow theory.

Improved thrust and drag performance was obtained by modifying the aft-end design of five selected air superiority fighters having twin buried engines and dual nozzles. The rationale for these modifications was derived from the predesign guidelines developed during the program. Improvements in mission radius for a fixed TOGW aircraft were obtained, in general, by utilizing convergent-divergent nozzles, a horizontal wedge interfairing with the trailing edge at the exit plane of the nozzles, a single vertical stabilizer, and a narrow lateral nozzle spacing.

References

- ¹Glasgow, E. R., Santman, D. M., and Miller, L. D., et al, "Experimental and Analytical Determination of Integrated Airframe-Nozzle Performance," AFFDL-TR-72-101, Oct. 1972, Air Force Flight Dynamics Lab., Wright-Patterson Air Force Base, Ohio.
- ²Presz, W., "Experimental and Analytical Determination of Integrated Airframe-Nozzle Performance, Phase III Summary Report, Pratt & Whitney Aircraft Support Program," PWA-4503, July 1972, Pratt and Whitney Aircraft, East Hartford, Conn.
- ³"Program for Experimental and Analytical Determination of Integrated Airframe-Nozzle Performance, Phase I Interim Report," LR 24183, Dec. 1970, Lockheed-California Co., Burbank, Calif.
- ⁴Konarski, M., "Experimental and Analytical Determination of Integrated Airframe-Nozzle Performance, Phase I Summary Report, Pratt & Whitney Aircraft Support Program," PWA-4065, Nov. 1970, Pratt and Whitney Aircraft, East Hartford, Conn.
- ⁵Galigher, L. L., "Evaluation of Various Exhaust Nozzles at Free-Stream Mach Numbers from 0.6 to 3.0," AEDC-TR-70-256, Dec. 1970, Arnold Engineering Development Center, Tullahoma, Tenn.
- ⁶"Program for Experimental and Analytical Determination of Integrated Airframe-Nozzle Performance, Phase II Interim Report," LR 24830, Feb. 1972, Lockheed-California Co., Burbank, Calif.
- ⁷Presz, W., "Experimental and Analytical Determination of Integrated Airframe-Nozzle Performance, Phase II Summary Report, Pratt & Whitney Aircraft Support Program," PWA-4375, Feb. 1972, Pratt and Whitney Aircraft, East Hartford, Conn.
- ⁸Galigher, L. L., "Performance of Various Twin-Nozzle Afterbody Configurations of an Air Superiority Fighter-Type Model at Mach Numbers from 0.6 to 2.5," AEDC-TR-72-17, Feb. 1972, Arnold Engineering Development Center, Tullahoma, Tenn.
- ⁹Glasgow, E. R., Divita, J. S., Everling, P. C., and Laughrey, J. A., "Analytical and Experimental Evaluation of Performance Prediction Methods Applicable to Exhaust Nozzles," AIAA Paper 71-719, Salt Lake City, Utah, 1971.
- ¹⁰"Project Tailor-Mate Vehicle Conceptual Design Study," FZA-587-002, Sept. 1969, (Classified Secret), Fort Worth Div., General Dynamics Corp., Fort Worth, Texas.
- ¹¹Spreiter, J. R., "On Alternate Forms for the Basic Equations of Transonic Flow Theory," *Journal of Aeronautical Science*, Vol. 21, No. 1, 1954, p. 70.